Research Article

Synthesis of Nanocomposites based on Mesoporous Aluminosilicate and Polyethyleneimine (PEI) for siRNA Delivery: Potential Usefulness of the Synergistic Effect of Al^{3+} Ion and PEI on the siRNA Delivery Efficiency for Diseases Treatment

Rafaatossadat Badihi[1], Ali Mahmoudi[1*], Mohammad Reza Sazegar[1*], Khodadad Nazari[2]

[a]Faculty of Chemistry, North Tehran Branch, Islamic Azad University, Hakimiyeh, Tehran, Iran

[b]Future Bioenergy solutions Inc., 369-901 3rd Street West, North Vancouver BC, V7P 3P9, Canada

*Corresponding author: Ali Mahmoudi, Faculty of Chemistry, North Tehran Branch, Islamic Azad University, Hakimiyeh, Tehran, Iran.

Citation: Badihi R, Mahmoudi A, Sazegar MR, Nazari K. Synthesis of Nanocomposites Based on Mesoporous Aluminosilicate and Polyethyleneimine (PEI) for siRNA Delivery: Potential Usefulness of the Synergistic Effect of Al3+ Ion and PEI on the siRNA Delivery Efficiency for Diseases Treatment. Journal of Nanotechnology Research 4 (2021): 029-044.

Abstract

Several nanocomposites based on Mesoporous Silica Nanoparticles (MSN), aluminum ions, and Polyethyleneimine (PEI) were synthesized by the combination of the sol-gel and post-synthesis methods. These nanocomposites were mainly composed of MSN with the leading of Al and PEI species alone or in combination. The Al-MSN, MSN-PEI, and Al-MSN/PEI samples were characterized by using FT-IR, XRD, SEM, EDX, zeta potential, and nitrogen physisorption techniques. The potential of their RNA delivery was investigated by loading and releasing the siRNA in the phosphate buffer. The obtained results showed that the loading capacity of each sample is directly related to its zeta potential. The Al-MSN/PEI sample showed the highest siRNA adsorption capacity due to possessing the highest zeta potential resulted in the presence of the high electric charge of Al^{3+} and the cationic nature of PEI. Under

the optimized conditions, the Al-MSN/PEI sample showed the amount of 47.19 μg adsorption of siRNA for 1.0 mg of Al-MSN/PEI. The results of releasing siRNA exhibited the yields of 12, 20.4, 29.6, and 36.0 % for MSN, MSN-PEI, Al-MSN, and Al-MSN/PEI, respectively at room temperature for 120 min.

Keywords: Aluminosilicate; Mesoporous silica nanoparticles; polyethyleneimine; siRNA delivery

1. Introduction

Mesoporous silica nanoparticles (MSNs) form an outstanding class of nanomaterials when their interesting properties such as high surface areas, large pore size and volume, tunable porosity, and thermal stability are considered [1]. The modification of the MSNs able to increase the activity of MSNs in the adsorption process due to the generation of the active sites on the surface of MSN. Introduction of transition metal ions such as cobalt in the MSN frameworks can be modified the mesoporous structure through the sol-gel method or by the impregnation technique [2-9]. Generally, MSN exhibit specific surface areas around 1000 m^2g^{-1}, and this unique feature in combination with their high porosity provides a suitable platform for loading and delivery of large amounts of molecules [10-12]. Gene therapy has been recognized as one of the most potent therapies for the treatment of complex diseases such as cancer, cardiovascular disorders, and Alzheimer's disease [13-16]. Initiation and propagation of these diseases are based on the expression of certain genes that need to be silenced by the aid of small interfering RNA (siRNA) molecules. These are also known as

short interfering RNA or silencing RNA, a class of double-stranded RNA and non-coding RNA molecules. They are typically made of 20-27 base pairs in length. They interfere with the expression of specific genes with complementary nucleotide sequences by degrading mRNA after transcription. siRNA may serve as the most appropriate tool for short term silencing of the protein-coding genes. Such therapy requires efficient gene delivery to cells because naked nucleic acids alone are not capable of getting across cell membranes [17,18]. Recently, some interesting methods for gene delivery have been introduced that included inorganic nanoparticles, liposomes, and polymer-based nanomaterials [19-22]. The good biocompatibility of the silica-based nanoparticles makes them a promising candidate for gene delivery [23,24]. Today, the attempts on developing silica-based gene delivery carriers are concentrated on two general aspects like surface chemistry and particle structure. From a surface chemistry point of view, before nucleic acid loading, an early modification step is required because the silica surface is negatively charged under biologically related conditions [25]. Different modifiers such as metal ions [26], amino silanes [27], cationic polymers [28,29], and peptides [30] have been used to change the surface charge of MSN. The modifier improves the interaction between DNA and MSN by reducing the electrostatic repulsion. Much attention has been paid to the modification of mesoporous silica materials and the enhancement of their adsorption capacity. Prabhakar and co-workers studied the effect of amino-functional groups on the surface of mesoporous silica material and enhanced the DNA binding via

electrostatic interactions [31]. Keasberry et al. reported that the MSNs modified with polyamidoamine dendrimers have high adsorption capacity for plasmid DNA, and therefore have a higher ability to transfect HeLa cells [32]. Recently, MSN was modified with polyethylenimine-polyethylene glycol copolymers (PEI-PEG) and used as a co-deliver anticancer drug and siRNA into the breast cancer cells, in order to decrease the cells' potency to develop drug resistance [33]. In nanoparticle-based gene delivery systems, the nucleic acids were carried exclusively by the outer surface of the nanoparticles [34-37]. In recent years, Kumar and his co-workers synthesized a Mesoporous silica nanoparticle based enzyme for colon specific drug delivery through a natural carbohydrate polymer of guar gum capping. They showed that the MSN structure was remained after guar gum capping via non-covalent interaction. The result was manifested the release of 5-flurouracil as an anticancer drug in colon cancer cell lines in vitro which confirmed by biochemical assay and flow cytometry [38]. In another study, Wu et al., researched on the preparation of mesoporous polymer nanospheres (MPNs) as nanocarriers of B-cell lymphoma 2 (Bcl-2) small interference RNA (siRNA) for breast cancer treatment. The FA-targeted-Bcl-2-siRNA-loaded nanoparticles were prepared via a layer-by-layer assembly through the electrostatic interactions. These nanoparticles showed anticancer effect was increased on breast cancer (BC) cells by a significant sequence-specific inhibition of Bcl-2 mRNA expression in the BC cells by cancer cell apoptosis [39]. Folic acid-loaded magnetic SBA-15 that incorporated with quercetin were synthesized to investigate human colorectal carcinoma cells (HCT-116). This composite caused the tumour suppression, and triggered mitochondrial-dependent apoptosis via a redox-regulated cellular signalling system [40]. In this study, we synthesized some nanocomposites based on the MSN which modified with aluminium, and polyethyleneimine (PEI) as the potential carriers for siRNA delivery. Their structures were characterized by using XRD, FTIR, SEM, BET, and TEM methods. In addition, the ability of their RNA delivery was investigated through the release of siRNA in the phosphate buffer solution (PBS, pH = 7.2) at room temperature. The important point of this study is that the aim of this research is merely to synthesize a nanocomposite based on mesoporous aluminosilicate nanoparticles and PEI polymer that carrier the siRNA. This study indicates that this nanocomposite with PEI polymer can be a good carrier for siRNA, and only the release of siRNA in the different alkali, acidic, and neutral media has been investigated. Therefore here, biological studies of the in vitro and in vivo tests have not been done on this nanocomposite.

2. Experimental

2.1 Materials

Tetraethylorthosilicate (TEOS, 98%), cetyltrimethylammonium bromide (CTAB, 95%), aminopropyltriethoxysilane (APTES, 99%), phosphate buffer (pH = 7.2), sodium hydroxide (extra pure), polyethyleneimine (MW 10 kD), and ethanol (99%) were purchased from Sigma-Aldrich Co. The certain siRNA was purchased from Sinagene Co. (Tehran). All of the solvents

and reagents were used as received without further purification. Double distilled water was used in all of the experiments. Aluminium nitrate nine hydrate $(Al(NO_3)_3.9H_2O)$ was purchased from Merck Co.

2.2 Methods

2.2.1 Synthesis of mesoporous silica nanoparticles (MSN)

MSN samples were prepared according to the reported procedure [35]. A solution of CTAB (10 g) in double-distilled water (275 ml) was prepared at room temperature. Then a solution of 25% ammonia (54 ml) in ethanol (395 ml) was added to the above-mentioned solution and the mixture was stirred for 5 h. Finally, TEOS (45 ml) was added to the mixture and stirred for 8 h. The gel was aged for 8 h. The precipitate was then washed with water and ethanol (300 ml) of each sample, oven-dried, and finally calcined at 550 °C.

2.2.2 Synthesis of Aluminium-modified mesoporous silica nanoparticles (Al-MSN)

MSN (0.1 g) was added to 0.3 M $Al(NO_3)_3.9H_2O$ in double-distilled water (20 ml) and sonicated for 50 min. The mixture was then stirred at 70 ^{o}C for 5 h. Afterward, the precipitate was filtered and washed three times with water, oven-dried at 90 °C for 24 h, and finally calcined at 650 ^{o}C for 3h. The obtained sample was denoted as Al-MSN [41,42].

2.2.3 Synthesis of PEI-modified MSN and Al-MSN

The PEI-modified MSN and Al-MSN samples were obtained as follows: the amount of 5.0 mg

of each sample was dispersed into the absolute ethanol (1.0 mL) and sonicated for 15 min. Then polyethyleneimine (PEI, MW 10 kD, 2.5 mg) was added to the dispersion and the mixture was stirred at room temperature for 15 h. The PEI-modified particles were collected by centrifugation, washed with absolute ethanol and distilled water (3×10 ml), and finally dried at room temperature. The samples were denoted as MSN-PEI and Al-MSN/PEI.

2.2.4 siRNA loading and release

The amount of siRNA was loaded on the MSN surface and monitored by using a UV-vis spectrophotometer. Typically, 10 mg of each sample was added to 10 ml of a 150 μg/mL solution of the siRNA in PBS (pH 7.2) and stirred at room temperature for 2 h. At given time intervals, the amount of the adsorbed siRNA on each sample was determined at λmax of 260 nm. The release of the siRNA was studied on the concentrations of 1, 5, 25, 50, 75, 100, and 150 μg ml^{-1} of siRNA, in phosphate buffer solution at 260 nm. The siRNA concentration was calculated as: [siRNA] = 0.0192 × Abs(260) − 0.037, (R^2 = 0.998), where Abs(260) stands for the absorbance of the solution at 260 nm.

2.3. Characterization of the nanocomposites

Fourier-transform infrared (FT-IR) spectra were recorded using KBr disks on a Rayleigh, WQF-510 infrared spectrophotometer. Ultraviolet-visible (UV-vis) absorption spectra were recorded on a Varian Cary 100 spectrophotometer in quartz cuvettes. Zeta potential measurements were performed on a Zetasizer Nano ZS (Malvern, Instruments, and

Westborough, MA) with a backscattering detection at 173°. Powder X-ray diffraction (XRD) data were collected with a Philips PW 1830 diffractometer (Cu-Kα X-radiation, λ = 1.54 Å). SEM imaging was performed on a JEOL JEM-2100 transmission electron microscope. N_2 adsorption-desorption isotherms were measured at 77 K on a BELSORP MINI II instrument. Samples were degassed in a vacuum and annealed at 120 ˚C for at least 6h to remove moisture. The pore size distribution was evaluated by using the Barrett–Joyner–Halenda (BJH) model.

3. Results and Discussion

3.1 Characterizations of the nanocomposites

The FT-IR spectra of the MSN, Al-MSN, MSN-PEI, and Al-MSN/PEI samples are shown in Figure 1. The broad bands at about 3452 cm^{-1} are attributed to the O–H stretching vibrations of either silanol groups or adsorbed water [25-43]. The O-H and Si-O-Si bending vibrations have also appeared at 1640 cm^{-1}. The symmetric and asymmetric Si–O–Si stretching vibrations were observed around the region of 1082 and 802 cm^{-1}, respectively [25]. Two weak peaks of the C-H stretching vibrations are visible at about 2970 and 2890 cm^{-1} which are attributed to the presence of the PEI molecules in the MSN-PEI and Al-MSN/PEI samples [41-43]. Metal-oxide vibrations of either Si^{4+} or Al^{3+} species in tetrahedral holes also appeared at 467 cm^{-1} [43]. Although the C-N stretching vibrations of the PEI are anticipated to appear in the range of 1000-1250 cm^{-1}, these were overlapped with the strong peaks of the Si-O-Si vibrations [43]. It can be concluded that PEI modification was successfully achieved and no

considerable change in the metal-oxide bands were occurred.

The low and high angle XRD patterns for the MSN, Al-MSN, MSN-PEI, and Al-MSN/PEI are presented in Figure 2. In all cases, a broad peak was observed at about 22°, which originates from amorphous silica [2]. In the low angle XRD patterns, three diffraction peaks of 100, 110, and 200 were observed at 2.65°, 4.3°, and 4.8°, respectively, for the MSN (Figure 2A). These peaks are indicative of the mesoporous silica structure [36,37]. The intensity of these peaks were decreased after incorporating the metal and organic compounds which showed the less order mesoporous structure for these nanomaterials [2, 43]. The morphology of the MSN, MSN-PEI, Al-MSN, and Al-MSN/PEI samples was studied by SEM imaging (Figure 3). All of the samples were made of uniform spherical particles in the range of 70-180 nm [2]. It is also noteworthy that PEI treatment did not change the morphology of the products as it is evident from Figure 3b, and 3d. The presence and homogeneity distribution of Al ions in the Al-MSN/PEI sample were investigated by EDX and mapping, respectively. Figure 4a shows a homogeneous distribution of Al^{3+} in its mesoporous silica and Figure 4b is evidence of the presence of Si, O, and Al species in Al-MSN/PEI. The nitrogen adsorption-desorption isotherms and pore size distribution of the samples are shown in Figure 5. All of the samples showed a type IV isotherm with distinct H4 hysteresis loops in the p/p_0 range of 0.3-1.0 (Figure 5A). The narrow pore size distribution of the samples are observed around 1.2 nm (Figure 5B).
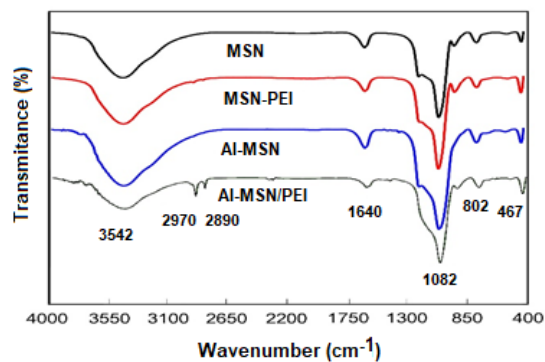
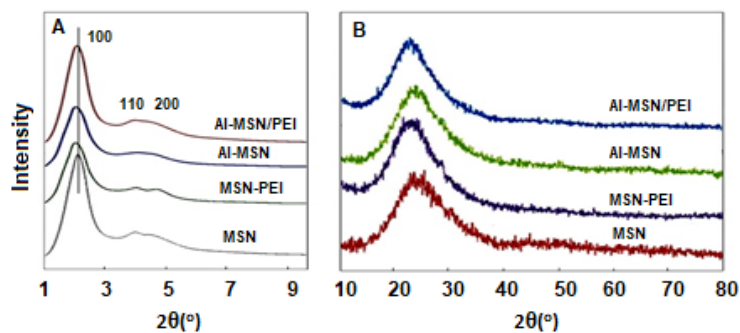**Figure 1:** FTIR spectra of the MSN, MSN-PEI, Al-MSN, and Al-MSN/PEI samples

Figure 2: XRD patterns of the MSN, MSN-PEI, Al-MSN, and Al-MSN/PEI samples (A) Low angle, and (B) high angle
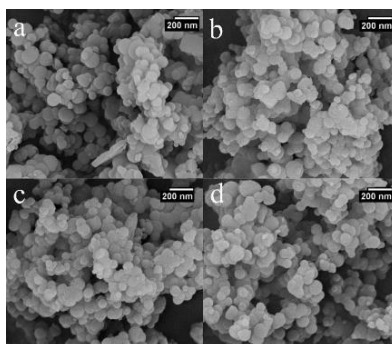

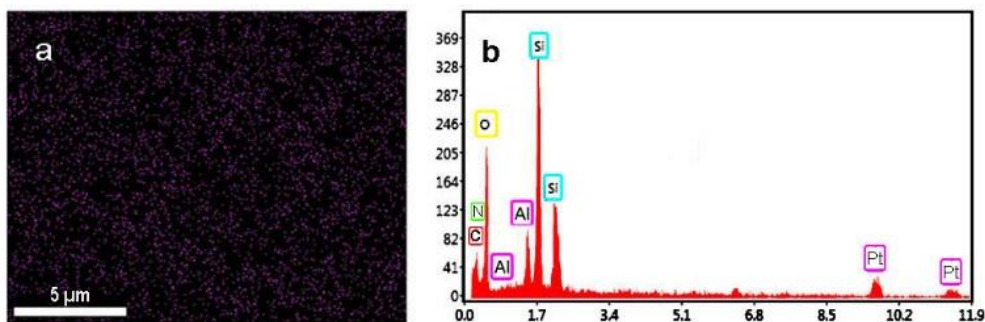**Figure 3:** SEM images of a) MSN, b) MSN-PEI, c) Al-MSN, and d) Al-MSN/PEI

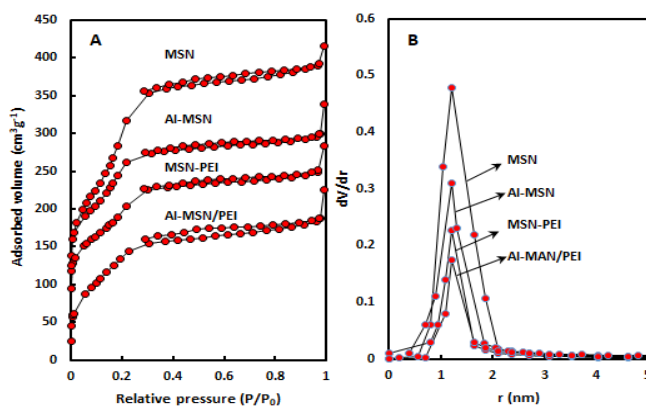**Figure 4:** Mapping (a), and EDX (b) analysis of the Al-MSN/PEI sample

Figure 5 (A): Nitrogen adsorption-desorption isotherms, **(B)** Pore size distributions of MSN, MSN-PEI, Al-MSN, and Al-MSN/PEI

Catalyst	S^a (m^2g^{-1})	V_p^b (cm^3g^{-1})	W^c(nm)
MSN	1062	0.53	2.00
Al-MSN	691	0.36	2.10
MSN-PEI	522	0.33	2.50
Al-MSN/PEI	393	0.34	3.44
^{a}S, Surface area obtained from N_2 adsorption-desorption isotherms; ^{b}V$_p$ Total pore volume; ^{c}W Pore diameter			

Table 1: Physicochemical properties of the MSN, MSN-PEI, Al-MSN, and Al-MSN/PEI samples.

The surface area of the MSN was reduced upon modification with either Al^{3+} or PEI (1062 m^2g^{-1} for MSN vs. 691, 552, and 393 m^2g^{-1} for the Al-MSN, MSN-PEI, and Al-MSN/PEI samples, respectively). Conversely, the total pore volume of the MSN was reduced after modification from 0.53 cm^3g^{-1} for MSN to 0.34 cm^3g^{-1} for Al-MSN/PEI which may be due to partial pore blockage by PEI, Al^{3+}, or both of them [6]. The pore size was also increased upon modification with Al^{3+} and PEI from 2.00 nm for MSN to 3.44 nm for Al-MSN/PEI.

3.2. Zeta potential measurements

Zeta potential of the synthesized samples is presented in Figure 6. The Zeta potential of the pure MSN was altered after introduction with aluminium ions and PEI species so the PEI-containing samples demonstrated positive zeta potentials [44]. The change in the zeta potential values from negative to positive indicated to increase in pure MSN surface isolation, due to the interactions between the MSN surface and PEI and aluminium ion modifiers [45]. The zeta potential of MSN was changed from −16.4 mV to 6.0 mV after amination with PEI, making it possible to load siRNA molecules through the electrostatic attractions. Metal ions are also known to increase siRNA adsorption onto silica surfaces due to the mediation of the electrostatic repulsion between the negatively charged silica surface and the siRNA molecule [46].

Higher zeta potential of Al-MSN (+26 mV) can be related to the electronic nature of the Al^{3+} ions which carries a high positive charge. PEI, on the other hand, is a cationic polymer which induces a very positive charge on the modified MSN. Thus, we decided to use a combination of PEI and Al^{3+} to obtain the highest possible zeta potential. As anticipated, Al-MSN/PEI showed a high zeta potential of 54.1 mV, which confirmed that trivalent metals bind more strongly to siRNA [47].
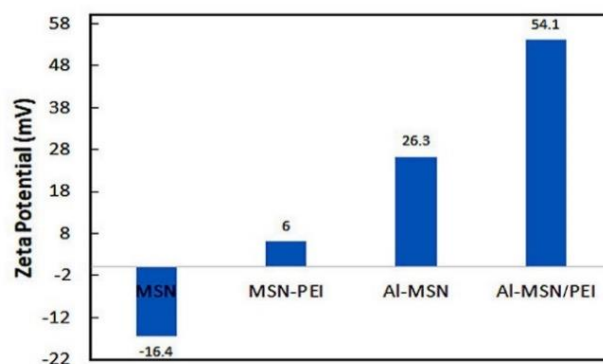

Figure 6: Zeta potential values of the MSN, MSN-PEI, Al-MSN, and Al-MSN/PEI

3.3. Loading and release of the siRNA

The trend of the siRNA incorporation on the MSN and its modified forms was studied by UV-vis spectroscopy. First, a calibration curve was plotted according to the method described under the heading 2.2.4 (Figure 7). (Figure 8) illustrates the trend of siRNA loaded after each 120 min for the MSN, Al-MSN, MSN-PEI, and Al-MSN/PEI samples. The adsorption capacity of the Al-MSN and MSN-PEI samples was higher than the pure MSN.

The adsorption capacity was improved when a combination of Al^{3+} and PEI was used. These observations are in agreement with the zeta potential values of the synthesized samples and the physicochemical properties (Table 1). The results showed although the MSN has the highest surface area and the highest monolayer adsorbed volume among the synthesized samples, it has the lowest siRNA adsorption capacity. Therefore, the adsorption capacity of the Al-MSN/PEI sample can be related to its physicochemical properties, including surface area, pore volume and pore diameter. Under the optimized conditions, 47.19 µg of the siRNA was loaded on 1.0 mg of the Al-MSN/PEI, after 90 min, which is a promising result. The siRNA release was investigated in a PBS (10 ml) at 260 nm, and at room temperature.

The results were calculated as $1- (A_1/A_0)$, where A_0 is the absorbance of the siRNA standard solution and A_1 is the absorbance of siRNA in the filtrate. Figure 9 depicts the trend of the siRNA release for 120 min from the Al-MSN, MSN-PEI, and Al-MSN/PEI samples. The sharp release of the siRNA was observed for all of the samples in the first 20 min. The pure MSN showed a release efficiency of about 13% of its initial siRNA loading after 120 min.

The MSN modification with aluminium or PEI alone or together had a significant positive effect on the release efficiency of the siRNA. The results showed 22, 30, and 36% siRNA release for the Al-MSN, MSN-PEI, and Al-MSN/PEI samples, respectively. According to the obtained results, the nanocomposite of Al-MSN/PEI exhibited the highest release due to the possessing the highest zeta potential on the surface of this composite. Since the MSN surface and the siRNA chain possess negative charge at neutral media [48], the pure MSN cannot strongly adsorb the siRNA chain due to the repulsion force between these two materials [49]. The formation of bonds occurred among the molecules with donor electron atoms and also phosphate groups in the siRNA chain with the Al^{3+} atoms in the nanomaterial structure [34]. The phosphate buffer solution reduced the interaction between the metal ions and the siRNA species which results in the release of the siRNA molecules.
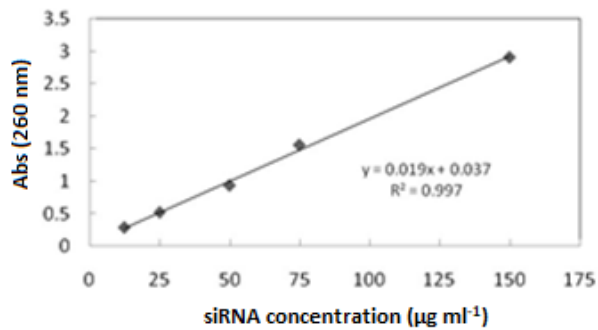
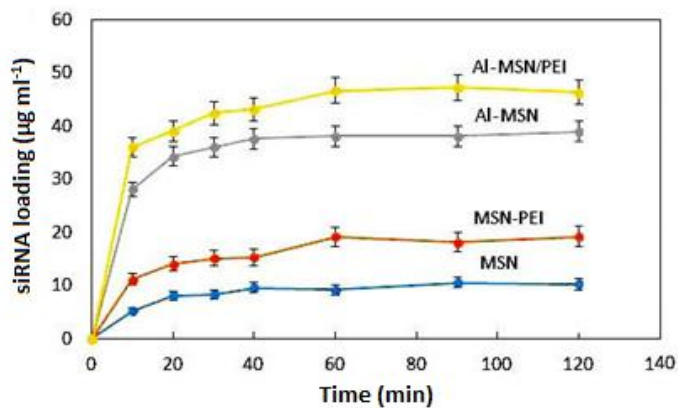**Figure 7:** The calibration curve for determination of the siRNA

Figure 8: Incorporation of the siRNA on the MSN, MSN-PEI, Al-MSN, and Al-MSN/PEI samples for 120 min
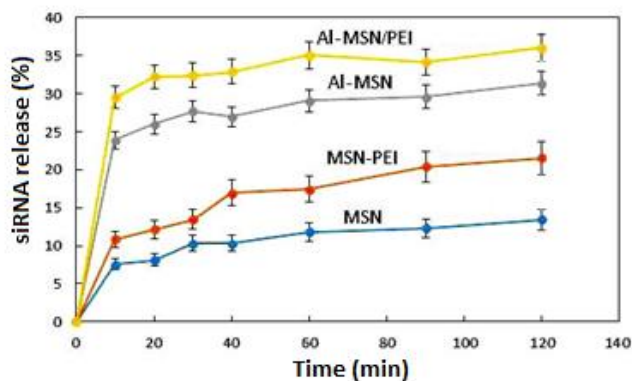

Figure 9: Desorption efficiency of the MSN, MSN-PEI, Al-MSN, and Al-MSN/PEI at room temperature for 120 min

According to the Hard and Soft Acids and Bases (HSAB) theory, hard acids tend to hard bases and soft acids prefer binding with the soft bases. Al^{3+} is known as a hard acid due to its high positive charge and small radius, and it can easily form a stable complex with a phosphate group of the siRNA molecule. It is worth noting that the siRNA delivery systems are actively pursued by researchers around the world. A comparison of our results with the reported methods on siRNA delivery is summarized in Table 2. In comparison with the other reported nanoparticles as siRNA carriers, Al-MSN/PEI nanoparticles show many advantages including ease of work-up, high performance in siRNA loading and release, and the use of affordable and non-toxic raw materials. The synthesized nanocomposites were able to undertake gene delivery in a high yield for the first time, and have superiority in comparison to the other reported nanomaterials. Another important advantage of our protocol is working at neutral pH. For example, calcium phosphate nanoparticles [53] as siRNA carriers need the pH of solution to be adjusted at 4.0.

Sample	Temp. (^{o}C)	Loading (%)	Release (%)	Ref.
Al-MSN/PEI	25	31.4	36	This study
Mannitol	25	2	2	50
Human Serum Albumin	37	8	40	51
PLGA	25	2	57	52
Chitosan nanoparticles (Ionic cross-linking)	25	8.3	9.5	53
Chitosan nanoparticles (Ionic gelation with TPP)	25	10	12	53
Mesoporous glass nanoparticles	25	2.5	40	54
Titania Nanotubes	25	2.2	90	55
Calcium phosphate nanoparticles	25	-	30	56

Table 2: A comparison of modified MSNs with the other vehicles for the siRNA delivery.

4. Conclusion

Mesoporous silica nanomaterials were synthesized and modified with aluminium and polyethyleneimine (PEI) to obtain suitable scaffolds for delivery of the siRNA chain. All of the synthesized samples were characterized by various techniques such as FT-IR, SEM, EDX, XRD, BET analysis. Zeta potential measurements showed that the loading of aluminium ions and PEI molecules to the MSN nanoparticles increased the zeta potential of the synthesized nanomaterials. The observed release efficiency for the MSN, MSN-PEI, Al-MSN, and Al-MSN/PEI nanocomposites were 12, 20.4, 29.6, and 36%, respectively. Obviously, the Al-MSN/PEI nanocomposite showed the highest

release efficiency. Al-MSN/PEI showed the highest zeta potential and exhibits the highest adsorption capacities among the synthesized samples. It was also found that the efficiency of the siRNA release from Al-MSN/PEI is just as good as its adsorption.

The present study aimed to extend the applications of the mesoporous silica nanoparticles to the treatment of the deadly diseases of the 21st century, including Alzheimer's disease, cancer, AIDS, etc. Although the gene silencing mediated by double-stranded small interfering RNA (siRNA) has been widely investigated as a potential therapeutic approach, its usage is hampered by its rapid degradation and poor cellular uptake into cells in vitro or in vivo. Therefore, we used MSNs as a siRNA vector due to their advantages such as low toxicity and biocompatibility. The results of the present study may provide a practical solution for siRNA purification techniques. Additionally, the Al-MSN/PEI nanocomposite can be utilized in the treatment or monitoring of gene-related diseases. The essential purpose of this study is only to prepare a nanocomposite based on mesoporous aluminosilicate nanoparticles modified with PEI polymer that able to transfer the siRNA. The release of the loaded siRNA was studied in three conditions the alkaline, acidic, and neutral media. The results indicated that about 36% release of siRNA has happened. According to the obtained results, the certain siRNA can be loaded in the modified mesoporous silica nanomaterials which able to do certain gene delivery or for silencing some gene through this type of nanocomposite. To find the capability of this nanocomposite in the treatment of some diseases such as cancer,

inflammatory and etc. through the gene or drug delivery, it is necessary to carry out the in vitro and/or in vivo biological studies.

Acknowledgments

Conflicts of interest

The authors declare no conflicts of interest.

References

1. Sazegar MR, Mukti RR, Triwahyono S, et al. High activity of aluminated bifunctional mesoporous silica nanoparticles for cumene hydrocracking and measurement of molar absorption coefficient. New J Chem 39 (2015): 8006-8016.

2. Hajiagha NG, Mahmoudi A, Sazegar MR, et al. Synthesis of cobalt-modified MSN as a model enzyme: Evaluation of the peroxidatic performance. Microporous Mesoporous Mater 274 (2019): 43-53.

3. Todorova S, Parvulescu V, Kadinov G, et al. Metal states in cobalt- and cobalt–vanadium-modified MCM-41 mesoporous silica catalysts and their activity in selective hydrocarbons oxidation. Microporous Mesoporous Mater 113 (2008): 22-30.

4. Popova M, Szegedi A, Cherkezova-Zheleva Z, et al. Toluene oxidation on titanium-and iron-modified MCM-41 materials, Hazard. Mater. J 168 (2009): 226-232.

5. Choopan Tayefe H, Sazegar MR, Mahmoudi A, et al. Catalyzed Schiff Base Synthesis over Bifunctionalized Cobalt/Zinc-

Incorporated Mesoporous Silica Nanoparticles under UV Irradiation. J. Nanostruct 9 (2019): 712-722.

6. Jamshidi D, Sazegar MR. Antibacterial Activity of a Novel Biocomposite Chitosan/Graphite Based on Zinc-Grafted Mesoporous Silica Nanoparticles. Int. J. Nanomedicine 15 (2020): 871-883.

7. Ortiz-Martinez K, Guerrero-Medina KJ, Roman FR, et al. Transition metal modified mesoporous silica adsorbents with zero microporosity for the adsorption of contaminants of emerging concern (CECs) from aqueous solutions. Chem Engin J 264 (2015): 152-164.

8. Vejdani Noghreiyan A, Sazegar MR, Mousavi Shaegh SA, et al. Investigation the emission spectra and cytotoxicity of TiO_2 and Ti-MSN/PpIX nanoparticles to induce photodynamic effects using X-ray. Photodiagn. Photodyn. Ther 30 (2020): 101770.

9. Sazegar MR, Dadvand A, Mahmoudi A. Novel protonated Fe-containing mesoporous silica nanoparticle catalyst: excellent performance cyclohexane oxidation. RSC Adv 7 (2017): 27506-27514.

10. Tang F, Li L, Chen D. Mesoporous Silica Nanoparticles: Synthesis, Biocompatibility and Drug Delivery. Adv. mater 24 (2012): 1504-1534.

11. Trofimov AD, Ivanova AA, Zyuzin MV, et al. Porous inorganic carriers based on silica, calcium carbonate and calcium phosphate for controlled/modulated drug delivery: Fresh outlook and future perspectives. Pharmaceutics 10 (2018): 167.

12. Baeza A, Ruiz-Molina D, Vallet-Regí M. Recent advances in porous nanoparticles for drug delivery in antitumoral applications: inorganic nanoparticles and nanoscale metal-organic frameworks. Expert opin. drug deliv 14 (2017): 783-796.

13. Verma IM, Naldini L, Kafri T, et al. Gene therapy: promises, problems and prospects. Genes and Resistance to Disease, Springer 2000: 147-157.

14. Pena SA, Iyengar R, Eshraghi RS, et al. Gene therapy for neurological disorders: challenges and recent advancements. J. Drug Target 28 (2020): 111-128.

15. Wang K, Kievit FM, Zhang M. Nanoparticles for cancer gene therapy: Recent advances, challenges, and strategies. Pharmacol. Res 114 (2016): 56-66.

16. Junquera E, Aicart E. Recent progress in gene therapy to deliver nucleic acids with multivalent cationic vectors. Adv. colloid interface sci 233 (2016): 161-175.

17. Kim MH, Na HK, Kim YK, et al. Facile synthesis of monodispersed mesoporous silica nanoparticles with ultralarge pores and their application in gene delivery. ACS nano 5 (2011): 3568-3576.

18. Chen J, Guo Z, Tian H, et al. Production and clinical development of nanoparticles for gene delivery. Ther M Methods Clin. Dev 3 (2016): 16023.

19. Zeng H, Little HC, Tiambeng TN, et al. Multifunctional dendronized peptide polymer platform for safe and effective siRNA delivery. Am J Chem. Soc 135 (2013): 4962-4965.

20. Zhang Y, Ren K, Zhang X, et al. Photo-tearable tape close-wrapped upconversion nanocapsules for near-infrared modulated

efficient siRNA delivery and therapy. Biomaterials 163 (2018): 55-66.

21. Van Bruggen C, Hexum JK, Tan Z, et al. Nonviral Gene Delivery with Cationic Glycopolymers. Acc. Chem. Res 52 (2019): 1347-1358.

22. Li Z, Zhang Y, Feng N. Mesoporous silica nanoparticles: synthesis, classification, drug loading, pharmacokinetics, biocompatibility, and application in drug delivery. Expert opin. drug deliv 16 (2019): 219-237.

23. Zhou Y, Quan G, Wu Q, et al. Mesoporous silica nanoparticles for drug and gene delivery. Acta pharm. Sin. B 8 (2018): 165-177.

24. Shao D, Lu Mm, Zhao Yw, et al. The shape effect of magnetic mesoporous silica nanoparticles on endocytosis, biocompatibility and biodistribution. Acta biomater 49 (2017): 531-540.

25. Niu B, Zhou Y, Wen T, et al. Proper functional modification and optimized adsorption conditions improved the DNA loading capacity of mesoporous silica nanoparticles. Colloids Surf. A Physicochem. Eng. Asp 548 (2018): 98-107.

26. Kamarudin NHN, Jalil AA, Triwahyono S, et al. Elucidation of acid strength effect on ibuprofen adsorption and release by aluminated mesoporousilica nanoparticles. RSC Adv 5 (2015): 30023-30031.

27. Topuz F, Uyar T. Cyclodextrin-assisted synthesis of tailored mesoporous silica nanoparticles. Beilstein J. Nanotechnol 9 (2018): 693-703.

28. Vathyam R, Wondimu E, Das S, et al. Improving the adsorption and release capacity of organic-functionalized mesoporous materials to drug molecules with temperature and synthetic methods. J. Phys. Chem. C 115 (2011): 13135-13150.

29. Lo KH, Chen MC, Ho RM, et al. Pore-filling nanoporous templates from degradable block copolymers for nanoscale drug delivery. Acs Nano 3 (2009): 2660-2666.

30. Cheng YJ, Zhang AQ, Hu JJ, et al. Multifunctional peptide-amphiphile end-capped mesoporous silica nanoparticles for tumor targeting drug delivery. ACS Appl. Mater. Interfaces 9 (2017): 2093–2103.

31. Prabhakar N, Zhang J, Desai D, et al. Stimuli-responsive hybrid nanocarriers developed by controllable integration of hyperbranched PEI with mesoporous silica nanoparticles for sustained intracellular siRNA delivery. Int. J. Nanomedicine 11 (2016): 6591.

32. Keasberry N, Yapp C, Idris A. Mesoporous silica nanoparticles as a carrier platform for intracellular delivery of nucleic acids. Biochemistry (Moscow) 82 (2017): 655-662.

33. Teo PY, Cheng W, Hedrick JL, et al. Co-delivery of drugs and plasmid DNA for cancer therapy. Adv. Drug Deliv. Rev 98 (2016): 41-63.

34. Jiang S, Zhuang J, Wang C, et al. Highly efficient adsorption of DNA on Fe^{3+} iminodiacetic acid modified silica particles. Colloids Surf. A Physicochem. Eng. Asp 409 (2012): 143-148.

35. Sazegar MR, Jalil AA, Triwahyono S, et al. Protonation of Al-grafted mesostructured silica nanoparticles (MSN):Acidity and catalytic activity for cumene conversion. Chem. Eng. J 240 (2014): 352-361.

36. Mahfoozi F, Mahmoudi A, Sazegar MR, et al. High-performance photocatalytic degradation of neutral red over cobalt grafted-mesoporous

silica under UV irradiation. J Sol-Gel Sci Technol 100 (2021): 170-182.

37. Sazegar MR, Mahmoudian S, Mahmoudi A, et al. Catalyzed Claisen–Schmidt reaction by protonated aluminate mesoporous silica nanomaterial focused on the (E)-chalcone synthesis as a biologically active compound. RSC adv 6 (2016): 11023-11031.

38. Kumar B, Kulanthaivel S, Mondal A, et al. Mesoporous silica nanoparticle based enzyme responsive system for colon specific drug delivery through guar gum capping. Colloids and Surfaces B: Biointerfaces 150 (2017): 352-361.

39. Wu X, Zheng Y, Yang D, et al. A strategy using mesoporous polymer nanospheres as nanocarriers of Bcl-2 siRNA towards breast cancer therapy, J. Mater. Chem. B 7 (2019): 477-487.

40. Mishra S, Manna K, Kayal U, et al. Folic acid-conjugated magnetic mesoporous silica nanoparticles loaded with quercetin: a theranostic approach for cancer management. RSC Adv 10 (2020): 23148-23164.

41. Babaei M, Eshghi H, Abnous K, et al. Promising gene delivery system based on polyethylenimine-modified silica nanoparticles. Cancer gene ther 24 (2017): 156-164.

42. Ma Z, Guan Y, Liu H. Superparamagnetic silica nanoparticles with immobilized metal affinity ligands for protein adsorption. Magn J. Magn Mater 301 (2006): 469-477.

43. Sun XY, Li PZ, Ai B, et al. Surface modification of MCM-41 and its application in DNA adsorption. Chin. Chem. Lett 27 (2016): 139-144.

44. Akbarzadeh M, Oskuee RK, Gholami L, et al. BR2 cell penetrating peptide improved the transfection efficiency of modified polyethyleneimine. J. Drug Deliv. Sci. Technol 53 (2019): 101154.

45. Lindén JB, Larsson M, Kaur S, et al. Glutaraldehyde-crosslinking for improved copper absorption selectivity and chemical stability of polyethyleneimine coatings. Appl J Poly. Sci (2016): 133.

46. Ganguly A, Ganguli AK. Anisotropic silica mesostructures for DNA encapsulation. Bull. Mater. Sci. 36 (2013): 329-332.

47. Zhang X, Zhang J, Quan G, et al. The Serum-Resistant Transfection Evaluation and Long-Term Stability of Gene Delivery Dry Powder Based on Mesoporous Silica Nanoparticles and Polyethyleneimine by Freezing-Drying. AAPS Pharm. Sci. Tech 18 (2017): 1536-1543.

48. He XX, Wang K, Tan W, et al. Bioconjugated Nanoparticles for DNA Protection from Cleavage. Am J Chem. Soc 125 (2003): 7168-7169.

49. Fujiwara M, Yamamoto F, Okamoto K, et al. Adsorption of Duplex DNA on Mesoporous Silicas: Possibility of Inclusion of DNA into Their Mesopores. Anal. Chem 77 (2005): 8138-8145.

50. Chow MY, Qiu Y, Lo FF, et al. Inhaled powder formulation of naked siRNA using spray drying technology with l-leucine as dispersion enhancer. Int. J. Pharm 530 (2017): 40-52.

51. Chow MYT, Qiu Y, Liao Q, et al. Porous and highly dispersible voriconazole dry powders produced by spray freeze drying for pulmonary delivery with efficient lung deposition. Int. J. Pharm 572 (2019): 118818-118829.

52. Cun D, Jensen DK, Maltesen MJ, et al. High loading efficiency and sustained release of siRNA encapsulated in PLGA nanoparticles: Quality by design optimization and characterization. Eur. J. Pharm. Biopharm 77 (2011): 26-35.

53. Katas H, Alpar HO. Development and characterisation of chitosan nanoparticles for siRNA delivery. J. Control. Release 115 (2006): 216-225.

54. ElpFiqi A, Kim TH, Kim M, et al. Capacity of mesoporous bioactive glass nanoparticles to deliver therapeutic molecules. Nanoscale 4 (2012): 7475-7488.

55. Song W, Zhao L, Fang K, et al. Biofunctionalization of titanium implant with chitosan/siRNA complex through loading-controllable and time-saving cathodic electrodeposition. J. Mater. Chem. B, 3 (2015): 8567-8576.

56. Li J, Chen YC, Tseng YC, Mozumdar S, Huang L. Biodegradable calcium phosphate nanoparticle with lipid coating for systemic siRNA delivery. J. Control Release 142 (2010): 416-421.